Hindawi Publishing Corporation
Advances in Civil Engineering
Volume 2009, Article ID 312034, 13 pages
doi:10.1155/2009/312034

Research Article

Effectiveness of Vehicle Weight Estimation from Bridge Weigh-in-Motion

Teerachai Deesomsuk and Tospol Pinkaew

Department of Civil Engineering, Chulalongkorn University, Phatumwan, Bangkok 10330, Thailand

Correspondence should be addressed to Tospol Pinkaew, tospol.p@chula.ac.th

Received 18 July 2009; Accepted 2 November 2009

Recommended by Ayman Mosallam

The effectiveness of vehicle weight estimations from bridge weigh-in-motion system is studied. The measured bending moments of the instrumented bridge under a passage of vehicle are numerically simulated and are used as the input for the vehicle weight estimations. Two weight estimation methods assuming constant magnitudes and time-varying magnitudes of vehicle axle loads are investigated. The appropriate number of bridge elements and sampling frequency are considered. The effectiveness in term of the estimation accuracy is evaluated and compared under various parameters of vehicle-bridge system. The effects of vehicle speed, vehicle configuration, vehicle weight and bridge surface roughness on the accuracy of the estimated vehicle weights are intensively investigated. Based on the obtained results, vehicle speed, surface roughness level and measurement error seem to have stronger effects on the weight estimation accuracy than other parameters. In general, both methods can provide quite accurate weight estimation of the vehicle. Comparing between them, although the weight estimation method assuming constant magnitudes of axle loads is faster, the method assuming time-varying magnitudes of axle loads can provide axle load histories and exhibits more accurate weight estimations of the vehicle for almost of the considered cases.

1. Introduction

The weights of vehicles govern the design requirements for highway infrastructure such as pavements and bridges. The traditional weigh stations are commonly used to weigh vehicles and impose fines or penalties for exceeding weight limits. They, however, take quite long time to weigh each vehicle. Moreover, their costs of system installation and maintenance are expensive. Therefore new alternative weigh system, namely, bridge weigh-in-motion (B-WIM) is developed. The bridge WIM systems deal with an existing instrumented bridge or culvert from the road network. Beside its cost advantage, the system installation and maintenance do not disturbed the traffic flow. In addition, the system is transparent to the vehicle's drivers so that the obtained weight information is expected to be unbiased. In general, B-WIM system monitors the deflection, strain, or bending moment data of the bridge during the passages of vehicles. Knowing the physical parameters of the bridge such as span length and flexural rigidity, the system can estimate the weights of passing vehicles from those bridge response data coupled with the configuration and speed information of vehicles which are obtained from another set of sensors. Based on previous researches, although many techniques have been proposed for bridge WIM to estimate the weights of vehicles, two different assumptions of vehicle loads on the bridge, which is either constant or time-varying moving loads, are often employed.

For the constant moving loads assumption, the vehicle is assumed to pass the bridge without any vertical body motion. Therefore, dynamic moving loads from vehicle exerting on the bridge can be simply replaced by constant moving loads. The weight estimation methods, in this class of assumption, determine axle weights of the vehicle by comparing the measured bridge responses with those obtained from bridge influence lines [1–6]. The determined individual axle weights are then added together to estimate the gross weight of vehicle. Since the vehicle is assumed

to be constant moving loads, the dynamic effects of the vehicle-bridge system significantly affect the accuracy of the estimated vehicle weights. Consequently, some latter research works employ a digital filtering technique to eliminate dynamic effects and reconstruct quasistatic responses of the bridge from measured bridge responses [7–9]. Although using these quasistatic responses yields more accurate weight estimation, the difficulty in selection of the proper filtering parameters and the cutoff frequency makes the method impracticable.

Similar to many load identification methods, the vertical body motion of vehicle induced by vehicle-bridge dynamic interaction is allowed. Therefore, unlike the constant loads assumption, the dynamic moving loads from vehicle exerting on the bridge are represented by time-varying loads moving on the bridge and are estimated directly from measured bridge responses. Then the axle weights of vehicle are determined from time averaging of the obtained time-varying axle loads. Many loads identification methods such as the time domain, the frequency-time domain, and the modal methods have been proposed and studied [10–13]. To obtain the estimated axle loads, the solution methods using either pseudoinverse or singular value decomposition technique are often adopted. However, it is found that all three methods exhibit large fluctuation of the identified loads due to measurement noises and possess numerically ill-condition, especially when the axle load is on bridge supports. In addition, the methods consume long computing time due to the inversion of large system matrices. Therefore, the least-square method with smoothening term named the regularization method is employed [14, 15]. The discrete version of the method is also considered using the dynamic programming technique [16]. Besides the efficiency of computation, this method eliminates an ill-conditioned problem and provides better identified axle loads under noisy inputs. Unfortunately, the method needs an optimal regularization parameter in the identification process. To overcome this problem, the regularization method with the iterative technique called the updated static component (USC) technique is adopted [17, 18]. It has been numerically and experimentally shown that the regularization with USC technique can substantially improve the estimation accuracy over the conventional regularization. The studies were also extended to the continuous bridges [19–23]. The obtained results reveal the effectiveness of the loads identification methods of this class.

Most of the mentioned weight or load estimation methods have been studied to show their effectiveness and potential for real application. However, the comparison between them has not yet been established. Therefore, in this paper, the two weight estimation methods of the vehicles using the constant moving loads and time-varying moving loads assumptions are extensively considered. Based on numerical simulations, many effects of vehicle and bridge WIM system such as bridge discretization, sampling frequency, vehicle speed, bridge surface roughness, number of measuring sections, noise, axle spacing, and axle weight distribution are investigated.

2. Simulation of Vehicle-Bridge Responses

2.1. Vehicle Model. A passage of vehicle on a bridge WIM system is shown in Figure 1. The system composes of a vehicle moving at a constant speed (v) interacting with an instrumented bridge structure. The vehicle is modeled using 4 degrees of freedom consisting of vertical displacement (y_v), rotation of vehicle body (θ_v), vertical displacement of front axle suspension mass (y_1), and vertical displacement of rear axle suspension mass (y_2). The equations of motion of vehicle are derived using dynamic equilibrium of the vehicle system in each degree of freedom and can be expressed by

$$\mathbf{M_v}\ddot{\mathbf{Y}}(t) + \mathbf{C_v}\dot{\mathbf{Y}}(t) + \mathbf{K_v}\mathbf{Y}(t) = \mathbf{P_v}(t), \tag{1}$$

where

$$\mathbf{M_v} = \begin{bmatrix} m_v & 0 & 0 & 0 \\ 0 & I_v & 0 & 0 \\ 0 & 0 & m_1 & 0 \\ 0 & 0 & 0 & m_2 \end{bmatrix}, \tag{2}$$

$$\mathbf{C_v} = \begin{bmatrix} C_{S1} + C_{S2} & (-C_{S1}a_1 + C_{S2}a_2)S & -C_{S1} & -C_{S2} \\ (-C_{S1}a_1 + C_{S2}a_2)S & (C_{S1}a_1^2 + C_{S2}a_2^2)S^2 & C_{S1}a_1S & -C_{S2}a_2S \\ -C_{S1} & C_{S1}a_1S & C_{S1} & 0 \\ -C_{S2} & -C_{S2}a_2S & 0 & C_{S2} \end{bmatrix}, \tag{3}$$

$$\mathbf{K_v} = \begin{bmatrix} K_{s1} + K_{s2} & (-K_{s1}a_1 + K_{s2}a_2)S & -K_{s1} & -K_{s2} \\ (-K_{s1}a_1 + K_{s2}a_2)S & (K_{s1}a_1^2 + K_{s2}a_2^2)S^2 & K_{s1}a_1S & -K_{s2}a_2S \\ -K_{s1} & K_{s1}a_1S & K_{s1} & 0 \\ -K_{s2} & -K_{s2}a_2S & 0 & K_{s2} \end{bmatrix}, \tag{4}$$

$$\mathbf{P_v}(t) = \begin{Bmatrix} 0 \\ 0 \\ P_f(t) \\ P_r(t) \end{Bmatrix} = \begin{Bmatrix} 0 \\ 0 \\ f_f(t) \\ f_r(t) \end{Bmatrix} + \begin{Bmatrix} 0 \\ 0 \\ N_f \\ N_r \end{Bmatrix}, \tag{5}$$

$$\mathbf{Y}(t) = \begin{Bmatrix} y_v(t) \\ \theta_v(t) \\ y_1(t) \\ y_2(t) \end{Bmatrix}, \tag{6}$$

$$\begin{aligned} f_f(t) &= K_{t1}\left(y_1 - \Delta_f\right) + C_{t1}\left(\dot{y}_2 - \dot{\Delta}_f\right), \\ f_r(t) &= K_{t2}(y_2 - \Delta_r) + C_{t2}(\dot{y}_2 - \dot{\Delta}_r), \end{aligned} \tag{7}$$

$$\begin{aligned} N_f &= (m_1 + a_2 m_v)g, \\ N_r &= (m_2 + a_1 m_v)g, \end{aligned} \tag{8}$$

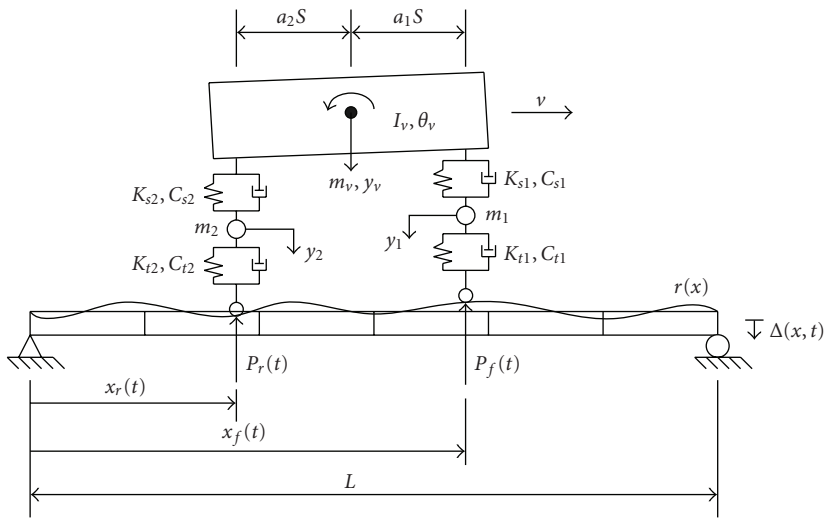

Figure 1: Vehicle and bridge WIM system.

while Δ_f and Δ_r are bridge deflections beneath front and rear axles of the vehicle, respectively.

2.2. Bridge Model. The bridge structure is modeled as a simply-supported bridge and is discretized by finite elements using beam element. The standard beam element having 2 nodes with 2 degrees of freedom in vertical displacement and rotation displacement at each node as shown in Figure 2 is adopted. The equations of bridge motion can be represented by

$$\mathbf{M_b}\ddot{\mathbf{u}}(t) + \mathbf{C_b}\dot{\mathbf{u}}(t) + \mathbf{K_b}\mathbf{u}(t) = \sum_{k=1}^{\mathrm{NE}} \mathbf{H}_k(\alpha(t))P(t), \tag{9}$$

where $\mathbf{u}(t)$, $\dot{\mathbf{u}}(t)$, and $\ddot{\mathbf{u}}(t)$ denote nodal bridge response vectors. $\mathbf{M_b}, \mathbf{C_b}$, and $\mathbf{K_b}$ are mass, damping, and stiffness matrices of the bridge, respectively. $\mathbf{H}_k(\alpha(t))$ is a matrix of global external load shape function used to transform the external front and rear axle loads $P(t) = [P_f(t) \quad P_r(t)]^T$ of the vehicle to the nodal loads on the bridge model, while $\alpha(t)$ is the distances of two axle loads on the beam element in local coordinates as in Figure 2 and NE is the total number of the beam elements.

2.3. Vehicle-Bridge Interaction Model. The vehicle-bridge interaction model can be formulated from the equations of vehicle motion (1), and the equations of bridge motion (9). Combining these equations through the force equilibrium of vehicle axle loads, the governing equations of the vehicle-bridge interaction system can be expressed by

$$\begin{bmatrix} \mathbf{M_b} & 0 \\ 0 & \mathbf{M_v} \end{bmatrix} \begin{Bmatrix} \ddot{\mathbf{u}}(t) \\ \ddot{\mathbf{Y}}(t) \end{Bmatrix} + \begin{bmatrix} \mathbf{C_b} + \overline{\mathbf{C}}_{11}(t) & -\mathbf{C_{12}}(t) \\ -\mathbf{C_{21}}(t) & \mathbf{C_v} + \mathbf{C_t} \end{bmatrix} \begin{Bmatrix} \dot{\mathbf{u}}(t) \\ \dot{\mathbf{Y}}(t) \end{Bmatrix} + \begin{bmatrix} \mathbf{K_b} + \overline{\mathbf{K}}_{11}(t) & -\mathbf{K}_{12}(t) \\ -\mathbf{K_{21}}(t) & \mathbf{K_v} + \mathbf{K_t} \end{bmatrix} \begin{Bmatrix} \mathbf{u}(t) \\ \mathbf{Y}(t) \end{Bmatrix} = \begin{Bmatrix} \mathbf{F_b}(t) \\ \mathbf{F_V}(t) \end{Bmatrix}, \tag{10}$$

where the matrices and variables contained in above equations are listed in the appendix.

It should be pointed out that the vehicle-bridge system forms a coupled time-varying dynamic system, because some elements in damping and stiffness matrices of the system keep changing with time due to a traveling of the vehicle.

To solve above equations, Newmark's β method is employed. Based on the obtained system responses, the bending moment of the bridge at any bridge section $m_j(t)$ as shown in Figure 2 can be determined from

$$m_j(t) = -\left(\frac{EI}{l^3}\right)\left\{\left(12\beta_j - 6l\right) \quad l\left(6\beta_j - 4l\right) \quad -\left(12\beta_j - 6l\right) \times l\left(6\beta_j - 2l\right)\right\} \times \left\{u_a(t) \quad u_b(t) \quad u_c(t) \quad u_d(t)\right\}^T, \tag{11}$$

where $u_a(t)$, $u_b(t)$, $u_c(t)$, and $u_d(t)$ are the obtained nodal displacements of the corresponding beam element and β_j is the local location of the measuring section determined from the global location x_j. In addition, the axle loads of vehicle can be determined from (5), (7), and (8) as

$$P(t) = \begin{Bmatrix} P_f(t) \\ P_r(t) \end{Bmatrix} = \begin{Bmatrix} K_{t1}\left(y_1 - \Delta_f\left(x_f\right) - r\left(x_f\right)\right) \\ +C_{t1}\left(\dot{y}_1 - \dot{\Delta}_f\left(x_f\right) - \dot{r}\left(x_f\right)\right) + (m_1 + a_2 m_v)g \\ K_{t2}\left(y_2 - \Delta_r(x_r) - r(x_r)\right) \\ +C_{t2}\left(\dot{y}_2 - \dot{\Delta}_r(x_r) - \dot{r}(x_r)\right) + (m_2 + a_1 m_v)g \end{Bmatrix}, \tag{12}$$

It is noted that these axle load equations take into account both static axle weights and their dynamic loads resulted from the vehicle-bridge interaction.

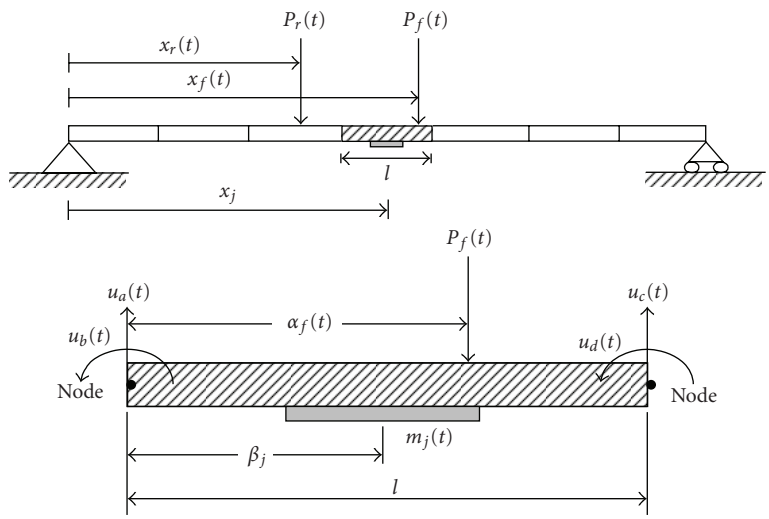

Figure 2: Bridge finite element model and local coordinates in beam element.

3. Weight Estimation of Vehicles

The concept of axle weight estimation of a passing vehicle is to minimize the error between measured and estimated bridge responses. In this paper, the measured bending moment vector $\mathbf{Z}(t)$ at N selected measuring points of the bridge under a moving vehicle is assumed to be simulated by solving the vehicle-bridge dynamic interaction (10) and introducing the obtained nodal bridge responses into (11). The corresponding estimated bending moment vector, $\hat{\mathrm{Z}}(\mathrm{t})$, at the same bridge sections is approximated by solving equations of motion of the bridge subjected to a pair of moving axle loads. In general, these axle loads are assumed to be either constant or time-varying magnitudes as will be discussed in the following sections. Then the moving axle loads of the vehicle are identified through the minimization of the square error of the bending moments of the bridge:

$$E = \sum_{i=1}^{\mathrm{NT}} \left[\left(\mathbf{Z}_i - \hat{\mathbf{Z}}_i \right)^T \mathbf{B} \left(\mathbf{Z}_i - \hat{\mathbf{Z}}_i \right) \right], \tag{13}$$

where $\mathbf{Z}_i = \{m_1 \ m_2 \ \ldots \ m_N\}_i^T$ and $\hat{\mathbf{Z}}_i = \{\hat{m}_1 \ \hat{m}_2 \ \ldots \ \hat{m}_N\}_i^T$ are discrete forms of measured and estimated bending moment vectors of the bridge at time step i, respectively.

$\mathbf{B}$ is the positive-definite weighting matrix and NT is the total number of data points (in time).

3.1. Method I: Constant Magnitude of Moving Axle Loads Assumption. With constant magnitude of moving axle loads assumption, the dynamic interaction loads between vehicle and bridge, that is, $f_f(t)$ and $f_r(t)$ as previously defined in (7), are assumed to be have zero mean and can be omitted for static weight estimation. Therefore the vehicle is simply replaced by a pair of constant static weights of moving axle loads as in Figure 3. To identify these constant axle loads of vehicle, the estimated bending moments of the bridge are calculated from static influence lines of moving loads and are compared with their corresponding measured bending moments. This method is simple but its main disadvantage is that it cannot provide any dynamic information of the axle loads of vehicle. The influence line of the bending moment of a simply-supported bridge at a section j as in Figure 3 can be expressed by a triangular function:

$$IL_j\ (x(t)) = \begin{Bmatrix} x(t) - \dfrac{x(t) \cdot x_j}{L}, & x(t) \le x_j \\ x_j - \dfrac{x(t) \cdot x_j}{L}, & x(t) > x_j \end{Bmatrix}, \tag{14}$$

where $IL_j\ (x(t))$ is the static influence line of bridge bending moment at measuring section j defined according to the load location, $x(t)$.

$x(t)$ is the distance of the moving front axle load, $x_f(t)$, or rear axle load, $x_r(t)$, from the left support of the bridge, and x_j is the distance of measuring section j from the left support of bridge.

Consequently, the estimated bending moment vector of the bridge at N measuring sections induced by the movement of front and rear axle loads can be computed by the method of superposition as

$$\begin{aligned} \hat{\mathbf{Z}}(t) &= \begin{Bmatrix} \hat{m}_1(t) \\ \hat{m}_2(t) \\ \vdots \\ \hat{m}_N(t) \end{Bmatrix} \\ &= \begin{Bmatrix} \hat{N}_f \cdot IL_1\left(x_f(t)\right) + \hat{N}_r \cdot IL_1(x_r(t)) \\ \hat{N}_f \cdot IL_2\left(x_f(t)\right) + \hat{N}_r \cdot IL_2(x_r(t)) \\ \vdots \\ \hat{N}_f \cdot IL_N\left(x_f(t)\right) + \hat{N}_r \cdot IL_N(x_r(t)) \end{Bmatrix}. \end{aligned} \tag{15}$$

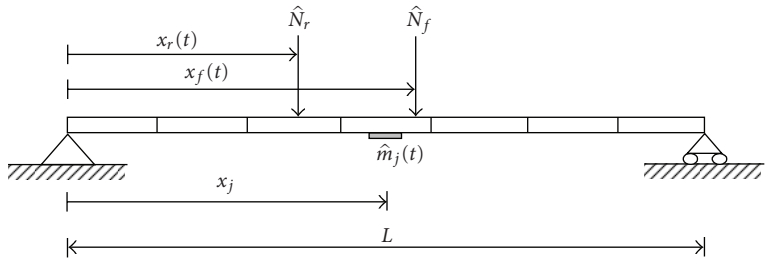

Figure 3: Model of a vehicle and bridge WIM system used for weight estimation with constant magnitude of moving loads assumption.

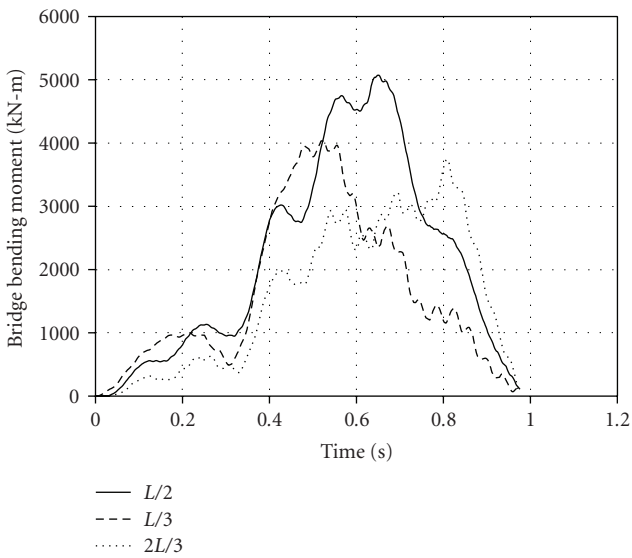

Figure 4: Typical bending moment histories of the bridge under a passage of the vehicle with a speed of 15 m/s and roughness surface of level 3.

Since the estimated bending moment of the bridge, $\hat{\mathbf{Z}}(t)$, depends on only a set of estimated moving axle weights, $\hat{N} = \{\hat{N}_f \quad \hat{N}_r\}$. Recalling (13), the objective function in term of time discretization can be rewritten as

$$E(\hat{N}) = \sum_{i=1}^{\mathrm{NT}} \left[\left(\mathbf{Z}_i - \hat{\mathbf{Z}}_i(\hat{N}) \right)^T \mathbf{B} \left(\mathbf{Z}_i - \hat{\mathbf{Z}}_i(\hat{N}) \right) \right]. \tag{16}$$

To minimize above objective function, $E(\hat{N})$, a Sequential Quadratic Programming (SQP) method is used. This method iteratively solves a series of quadratic programming (QP) problems, using the Broyden, Fletcher, Goldfarb, and Shanno (BFGS) formula to update the Hessian of the Lagrangian, $L(\hat{N})$:

$$L(\hat{N}) = E(\hat{N}) + \sum_{k=1}^{2} \gamma_k g_k(\hat{N}), \tag{17}$$

where $g_k(x)$ are the constraints including upper and lower bounds of axle weights, and γ_k are the Lagrange multipliers.

The MATLAB's optimization function *fmincon* [24], which utilizes previously mentioned procedures, is adopted to find the optimal axle weights, $\hat{N} = [\hat{N}_f \quad \hat{N}_r]^T$, which yields minimum error between the measured and the estimated bending moment vectors. These obtained optimal axle weights are constant and are assumed to be the best estimated axle weights for the passing vehicle.

3.2. Method II: Time-Varying Magnitude of Moving Axle Loads Assumption. Unlike the constant magnitudes of moving axle loads assumption, the axle loads of vehicle are assumed to be time-varying. With this assumption, the dynamic interaction loads between vehicle and bridge, that is, $f_f(t)$ and $f_r(t)$, as well as the static axle weights of vehicle, that is, $\hat{N}_f$ and $\hat{N}_r$, are taken into account. Therefore the vehicle is replaced by a pair of time-varying magnitudes of moving axle loads similar to the system shown in Figure 2. To identify the axle loads of vehicle, the estimated bending moments of bridge are calculated solely from the bridge equilibrium (9). Then the axle loads identification is accomplished through minimizing the output error between the measured and the estimated bridge responses using the conventional regularization expressed in time-discretization form [16] as

$$E(\hat{P}) = \sum_{i=1}^{\mathrm{NT}} \left(\mathbf{Z}_i - \hat{\mathbf{Z}}_i(\hat{P}) \right)^T \mathbf{B} \left(\mathbf{Z}_i - \hat{\mathbf{Z}}_i(\hat{P}) \right) + \lambda \hat{P}_i^T \hat{P}_i, \tag{18}$$

where $\hat{P} = [\hat{P}_f \quad \hat{P}_f]^T$ is the unknown moving loads vector with time-varying magnitude at time step i and λ is the regularization parameter.

In this paper, the dynamic programming method with updated static component technique [17] is employed to minimize above error equation. This is because the method yields better solution and robustness against the choice of λ than the conventional regularization method. It is noted that the obtained axle loads, $\hat{P}$, from (18) are time-varying loads. Therefore, to estimate the corresponding axle weights of vehicle, the simple time-averaging is adopted:

$$\hat{N}_f = \frac{1}{\mathrm{NT}} \sum_{i=1}^{\mathrm{NT}} \left[\hat{P}_f \right]_i, \qquad \hat{N}_r = \frac{1}{\mathrm{NT}} \sum_{i=1}^{\mathrm{NT}} \left[\hat{P}_r \right]_i \tag{19}$$

in which $\hat{N}_f$ and $\hat{N}_r$ are the estimated front and rear axle weights, respectively.

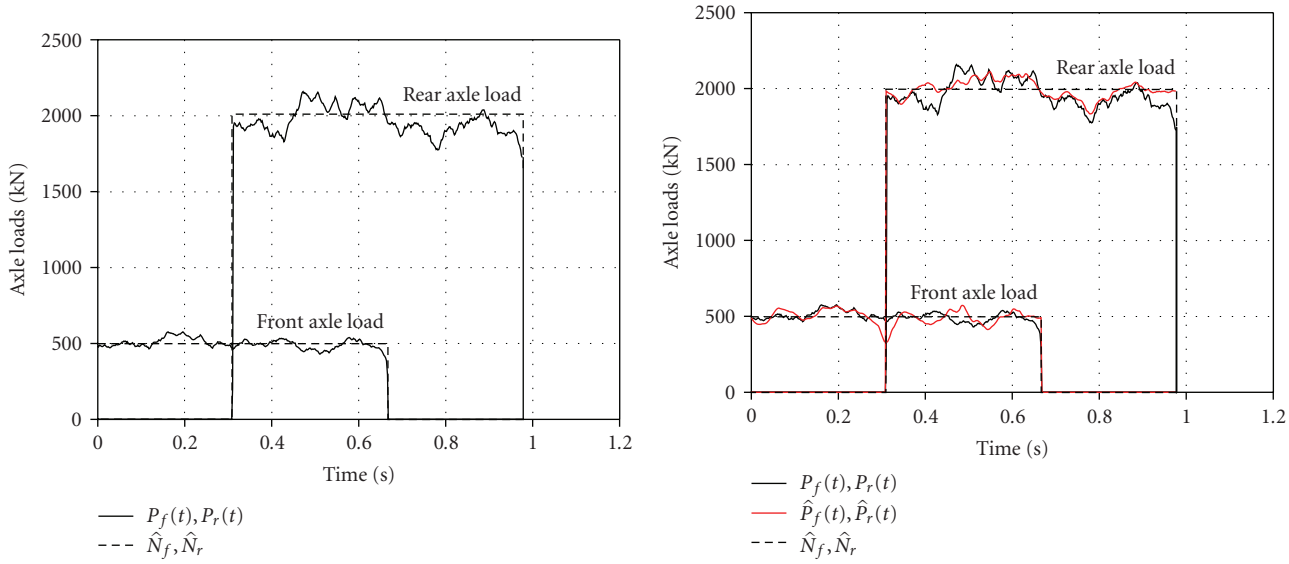

(a) Method I (b) Method II

Figure 5: Actual axle loads and corresponding axle weight estimations (a) using Method I and (b) using Method II.

Table 1: Parameters of vehicle and bridge WIM system.

Bridge	Vehicle		
$L = 10$ m	$I_v = 4.87$ kgm^2	$m_1 = 500$ kg	$m_2 = 700$ kg
$EI = 1.96\times10^9$ Nm^2	$m_v = 23800$ kg	$K_{s1} = 9.50\times10^6$ N/m	$K_{s2} = 16.98\times10^6$ N/m
$\rho A = 10.8$ kg/m	$S = 4.65$ m	$K_{t1} = 5.38\times10^6$ N/m	$K_{t2} = 12.82\times10^6$ N/m
$\xi = 0.02$ for all mode	$a_1 = 0.811$	$C_{s1} = 4.0\times10^4$ N/m/s	$C_{s2} = 4.0\times10^4$ N/m/s
	$a_2 = 0.189$	$C_{t1} = 4.0\times10^4$ N/m/s	$C_{t2} = 4.0\times10^4$ N/m/s

4. Numerical Examples

The numerical investigation of axle weight estimation of a passing vehicle on a bridge WIM system using the two previously mentioned methods is considered. The vehicle is assumed to have two axles and crosses the bridge with a constant speed. The bending moment histories of the instrumented bridge at various sections subjected to a passage of the vehicle are simulated from the vehicle-bridge interaction model as derived in (10). To reduce the simulation error, Newmark's β method with a fine time interval of 0.001 second is adopted to numerically determine bridge bending moments. Based on these obtained moment responses, the axle weights of the passing vehicle are estimated using either Method I or Method II. The weight estimations from the two methods are extensively investigated and the obtained results are compared under various conditions of vehicle-bridge parameters. To quantify the estimation accuracy of the methods, the weight estimation errors for the front and rear axles are, respectively, defined as

$$\text{Weight estimation error} = \frac{\hat{N}_f - N_f}{N_f} \times 100\%, \quad \frac{\hat{N}_r - N_r}{N_r} \times 100\%. \tag{20}$$

It is noted that the weighting matrices, **B**, defined in (16) for the Method I and (18) for the Method II are both set to identical matrix to prevent the bias comparison. It is also noted that the regularization parameter, λ, as required by (18) for the Method II is simply set to 1.0.

The parameters for the vehicle and bridge WIM system are listed in Table 1. The bridge structure is modeled as a simply supported beam having span length of 10 m. Its properties are approximated from a real concrete bridge in Thailand. It is noted that the first five natural frequencies of this bridge are computed to be 6.7, 26.8, 60.2, 107.1, and 167.3 Hz. The vehicle having gross weight of 250 kN is considered. Its dynamic properties are obtained from model identification by testing of a real two-axle 10-wheel truck.

Figure 4 shows typical bending moment histories of the bridge at $L/3$, $L/2$, and $2L/3$ under a passage of vehicle with speed of 15 m/s, respectively. Using these simulated bridge moment responses as the input, the axle weights of the vehicle can be estimated using Methods I and Method II as previously outlined and are shown in Figures 5(a) and 5(b), respectively. It should be noted that Method I yields directly the two axle weights of vehicle. On the other hand, Method II firstly yields the time-varying magnitudes of axle loads which can then be averaged to estimate the corresponding

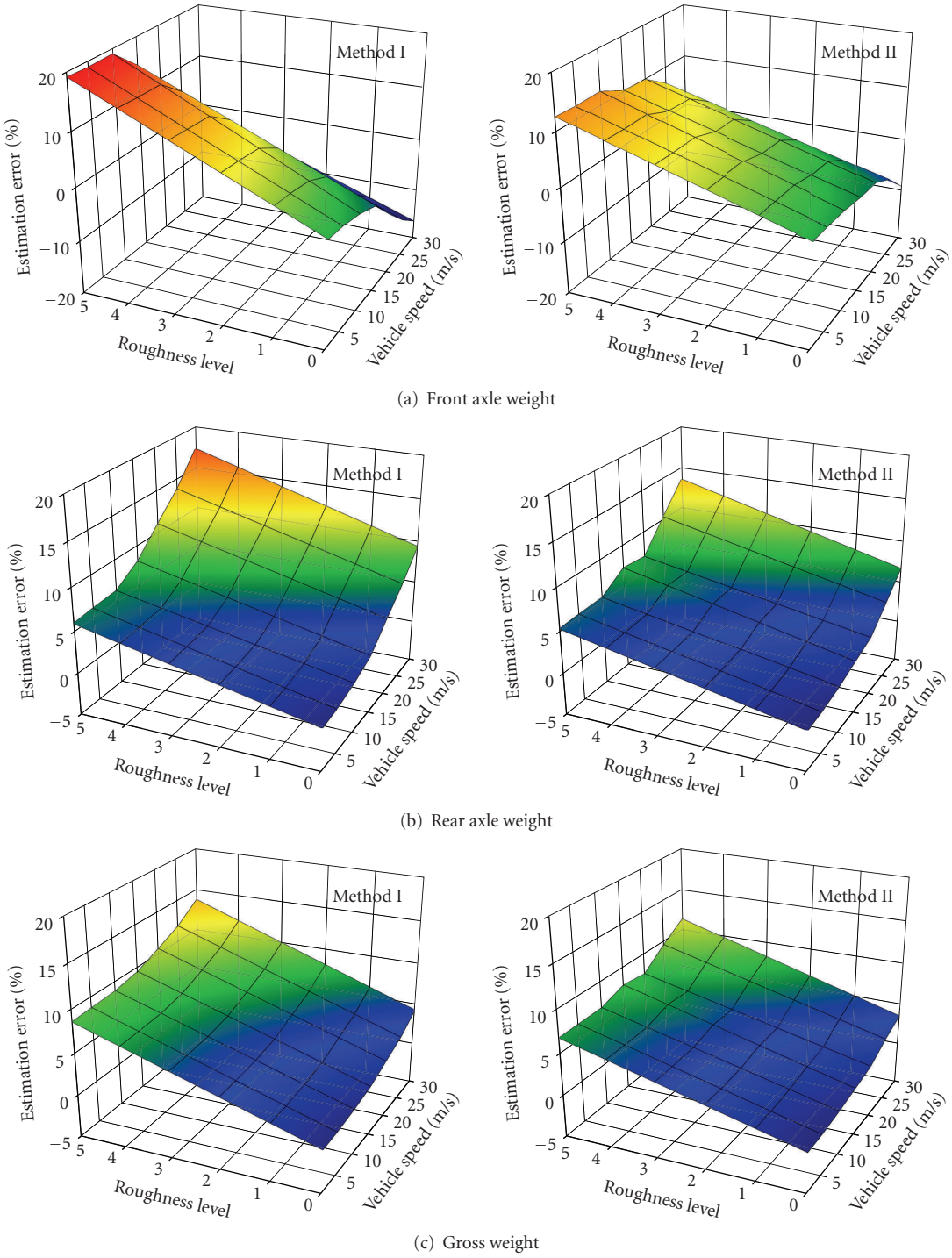

Figure 6: Estimation errors of axle weights under various roughness levels and vehicle speeds for (a) front axle weight, (b) rear axle weight, and (c) gross weight.

axle weights of vehicle. The figures clearly reveal that both methods can accurately estimate the front and rear axle, weights of vehicle. In this particular case, the estimation errors of the front axle, rear axle, and gross weights are, respectively, about 3.9, 4.4, and 4.3 using Method I and about 2.9, 3.7, and 3.5 using Method II.

4.1. Effects of Bridge Discretization and Sampling Frequency. The effects of bridge discretization and sampling frequency on the accuracy of the weight estimation methods are considered. The vehicle moving on the bridge at a constant speed of 15 m/s under various bridge discretization refinements and various sampling frequencies of bridge bending moments is

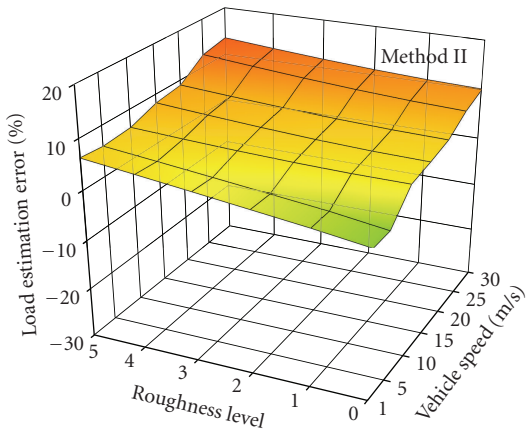

Figure 7: The rear axle load estimation error of vehicle load under various roughness levels and vehicle speeds using Method II.

Table 2: Estimation errors of axle weights for different sampling rate and number of beam elements.

Sampling Frequency (Hz)	Method I			Method II											
				Number of beam elements											
				4			8			12			16		
	front	rear	gross	front	rear	gross	front	rear	gross	front	rear	gross	front	rear	gross
20	−7.4	12.2	8.3	8.8	13.9	12.9	8.7	12.6	11.8	6.5	12.4	11.2	5.8	12.3	11
30	−9.5	12.1	7.8	−4.8	8.9	6.2	−0.3	8.1	6.4	1.7	8	6.7	2.7	7.8	6.8
40	−10	12.4	7.9	−0.9	7	5.4	−7.2	10.3	6.8	−6.6	11	7.4	−5.9	11	7.7
50	−10.3	12.6	8	−0.3	6.3	5.0	0.4	7.8	6.3	0.6	8.8	7.1	0.6	9	7.3
100	−10.3	12.6	8	−4.6	7.2	4.9	−2.9	8.9	6.5	−3.1	9.7	7.2	−2.8	9.9	7.4
200	−10	12.5	8	−7.9	9.4	5.9	−4.9	9.5	6.6	−3.6	9.8	7.1	−3.6	12.2	7.4
300	−10.1	12.5	8	−7.3	9.1	5.9	−4.9	9.5	6.6	−3.7	9.7	7	−3.7	10.1	7.3
400	−10	12.5	8	−7.8	9.5	6	−4.7	9.4	6.6	−3.6	9.7	7	−3.1	9.8	7.2
500	−10.1	12.5	8	−7.8	9.5	6	−4.6	9.4	6.6	−3.6	9.7	7	−3.1	9.8	7.2
1000	−10.1	12.5	8	−7.7	9.4	6	−4.5	9.3	6.6	−3.6	9.6	7	−3	9.7	7.2

Table 3: Measuring point arrangement.

Number of measuring points	Location arrangement
1	$1/2L$
3	$1/4L$, $1/2L$, $3/4L$
5	$1/8L$, $1/4L$, $1/2L$, $3/4L$, $7/8L$
7	$1/8L$, $1/4L$, $3/8L$, $1/2L$, $5/8L$, $3/4L$, $7/8L$
9	$1/8L$, $1/4L$, $3/8L$, $7/16L$, $1/2L$, $9/16L$, $5/8L$, $3/4L$, $7/8L$

simulated. Based on the obtained bridge moments at three sections, that is, $L/3$, $L/2$, and $2L/3$, the axle weights of the vehicle is estimated using Method I and Method II. Table 2 lists the estimation errors of front axle, rear axle, and gross weights of vehicle from the two methods. In the table, the simulated bending moments of bridge are sampled with the sampling frequency varied from 20 to 1,000 Hz. To estimate the axle weights of vehicle using Method II, the bridge structure is discretized into 4, 8, 12, and 16 beam elements. It should be noted that the bridge discretization

Table 4: Comparison on CPU processing times from the two methods.

Method	Method I			Method II		
	Min	Max	Avr.	Min	Max	Avr.
Total processing time (s)	1.2	2.6	1.8	3.6	10.8	6.5

for Method I is not necessary since the method utilizes the continuous influence line function. In the table, the bridge surface roughness of level 2, which induces the dynamic in axle loads around 10%, is also assumed.

Employing Method II, it is obviously found from the table that the accuracy of axle weight estimations is not affected by discretization refinement of bridge structure if it is discretized by more than 4 elements. The table also indicates that the accuracy of axle weight estimations by the two methods is significantly influenced by sampling frequency. The weight estimation errors become larger when the sampling frequency is smaller. However, the weight estimation errors obtained from both methods are rather constant if the sampling frequency is faster than around 50 Hz. Therefore, throughout this study, the number of

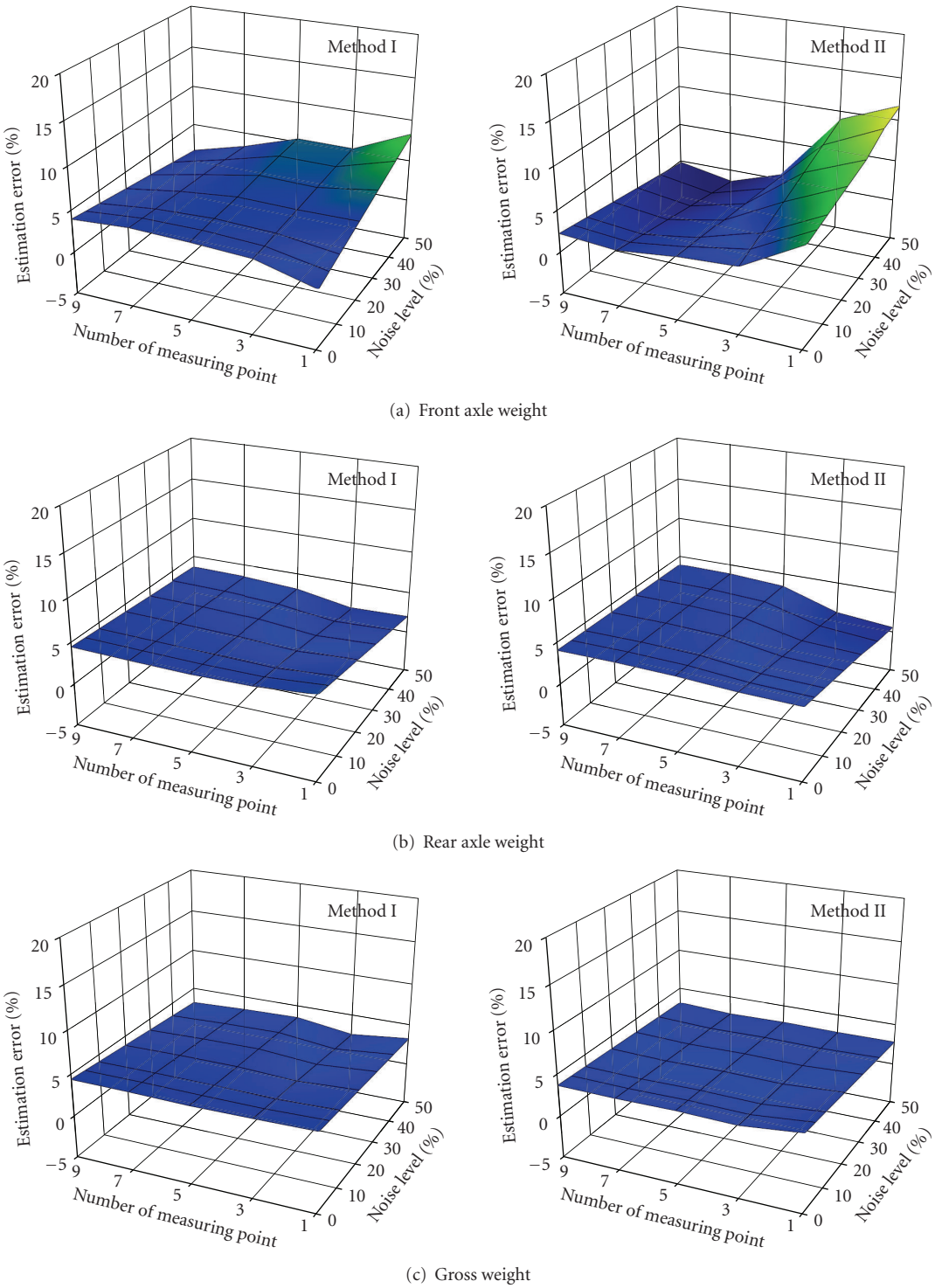

(a) Front axle weight

(b) Rear axle weight

(c) Gross weight

Figure 8: Estimation errors of axle weights under various numbers of measuring points and noise levels for (a) front axle weight, (b) rear axle weight, and (c) gross weight.

bridge elements is set to 8 while the sampling frequency is fixed at 500 Hz to guarantee the highest accuracy of the estimation methods. These imply that the bridge vibrations up to the 6th natural mode are taken into account. It is noted that these settings are used only for weight estimation methods. The vehicle-bridge interaction simulation of (10) still employs a very fine time interval of 0.001 second (1000 Hz) with 16 beam elements to accurately simulate the actual bending moments of the bridge WIM under a passage of vehicle.

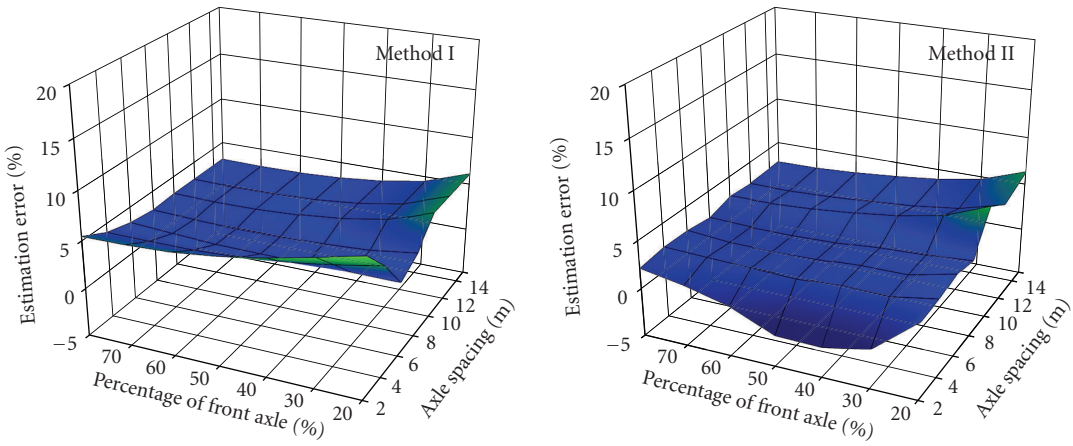

(a) Front axle weight

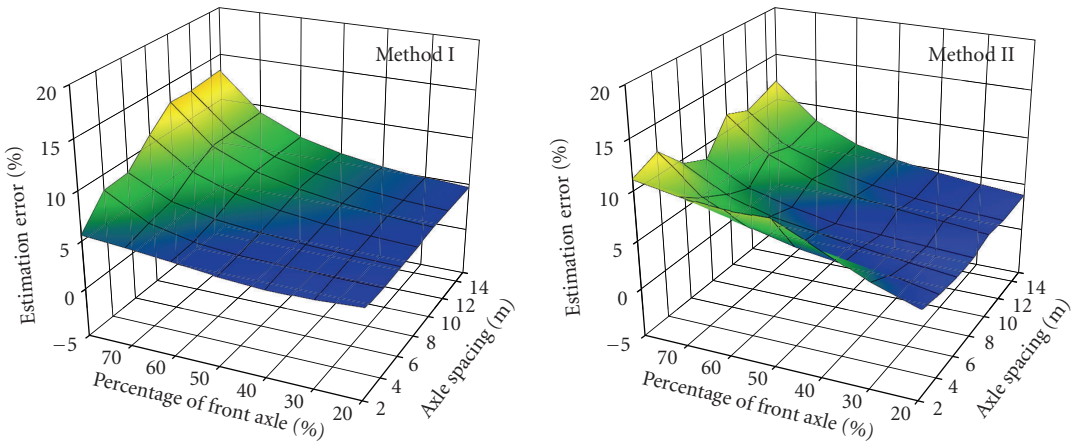

(b) Rear axle weight

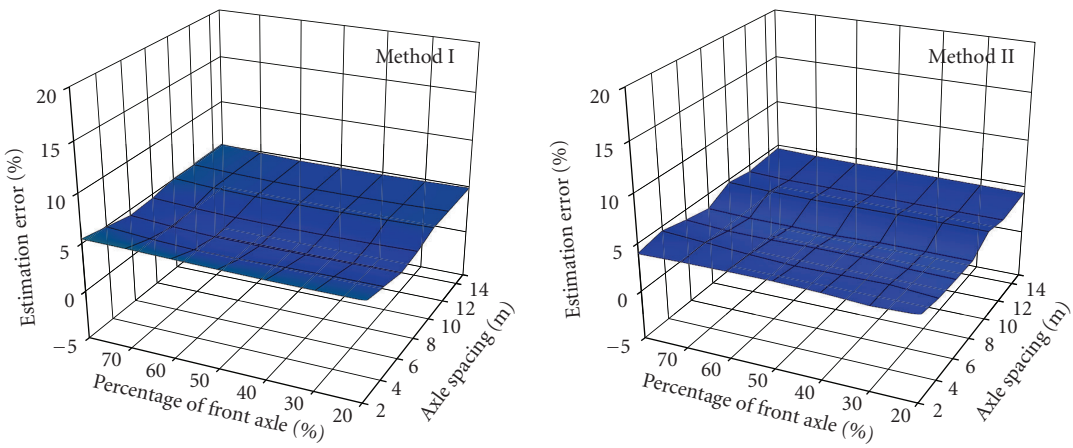

(c) Gross weight

Figure 9: Estimation errors of axle weights under various axle spacings and axle weight distributions for (a) front axle weight, (b) rear axle weight, and (c) gross weight.

4.2. Effects of Vehicle Speed and Bridge Surface Roughness. The effects of vehicle speed and bridge surface roughness on the accuracy of the weight estimation methods are investigated. The practical range of vehicle speed from 1 to 30 m/s is considered. The magnitude of bridge surface roughness, $|r(x)|$, is varied and is classified into 6 roughness levels ranging from 0 (smooth surface) to 5 (very rough surface) according to the obtained dynamic characteristic of the simulated axle loads. In general, roughness levels of 0, 1, 2, 3, 4, and 5 indicate the averaged dynamic participations in

each axle loads of vehicle moving at 15 m/s around 0%, 5%, 10%, 15%, 20%, and 25%, respectively. The vehicle moving on the bridge having different roughness levels at various speeds is simulated. Based on the obtained bridge moments at three sections, that is, $L/3$, $L/2$, and $2L/3$, the axle weights of vehicle are estimated using Method I and Method II. Figures 6(a) to 6(c) plot the estimation errors of front axle, rear axle, and total weights of vehicle from the two methods under various vehicle speeds and bridge roughness levels. For a better visualization, the weight estimation errors from Method I and Method II are separately plotted and shown in the left and right figures, respectively. These figures reveal that the weight estimation errors from both methods exhibit similar characteristic under variations of vehicle speed and bridge roughness level. It is found that their estimation errors tend to increase as the roughness level increases due to larger fluctuation of axle loads. Although the faster vehicle speed also induces larger fluctuation of axle loads, the speed effects on the estimation errors for front (Figure 6(a)) and rear axles (Figure 6(b)) become different. The former becomes smaller while the latter becomes larger when the vehicle speed increases. Since the rear axle is much heavier than the front axle, the estimation errors of gross weight from both methods (Figure 6(c)) are almost the same as those of the rear axle (Figure 6(b)). Comparing the errors from the two estimation methods, it is found from these figures that Method II is superior for all considered ranges of vehicle speeds and roughness levels. In particular, the estimation errors of front axle, rear axle, and gross weights using Method II are, respectively, varied from −9.26% to 12.53%, −0.20% to 13.51%, and −0.27% to 11.30% and using Method I are, respectively, varied from −16.38% to 19.20%, 0.02% to 17.31%, and 0.01% to 13.71%. It is observed from Figure 6(c) that the estimation errors of gross weight of vehicle from the two methods can be however controlled to be within ±10% if the surface roughness is kept below level 4, regardless to the vehicle speed.

Since Method II provides not only the estimated axle weight of vehicle but also its dynamic axle loads, it is therefore interesting to investigate the accuracy of identified dynamic axle loads of the method. To do so, the load estimation errors of rear axle defined by norm of the load error, $\|P(t) - \hat{P}(t)\|/\|P(t)\|$, are plotted in Figure 7 under various vehicle speeds and bridge roughness levels. It is noticed from the figure that the load estimation error is affected by both vehicle speed and bridge roughness level. The error increases as the vehicle speed or bridge roughness level increases. Based on considered ranges of speed and roughness level, the estimation errors of −0.55% to 13.49% are observed.

4.3. Effects of Number of Measuring Sections and Noise Level. The influences of number of measuring sections and noise levels in the input signals on weight estimation accuracy resulting from the two methods are investigated. The vehicle moving at a constant speed of 15 m/s on the bridge having roughness of level 3 is simulated. Based on the obtained bridge moments at various section arrangements as in Table 3, the axle weights of vehicle are estimated using Method I and Method II. It is noted that the number of the measuring sections of 1, 3, 5, 7, or 9 sections is considered. To study the noise effect, the obtained moment signals at all sections are assumed to be polluted with 5% to 50% white noise. Figures 8(a) to 8(c) show the estimation errors of front axle, rear axle, and gross weights of vehicle from the two methods under various number of measuring sections and noise levels. The results indicate that the influence of number of measuring sections and noise levels on weight estimation accuracy resulting from the two methods are very small, especially for rear axle and gross weights. Although both estimation methods are expected to be very robust against noise effect since their computations inherently contain time averaging procedure, the significant effect of noise on the weight estimation of front axle is observed when small number of measuring sections, that is, 1 or 3, is employed. It should be noted that both estimation methods can provide rather accurate weight estimation using only mid-span ($L/2$) bending moment as the input even though the number of vehicle axle is 2. This implies that the application of the two methods can be extended to the case where multiple vehicles are simultaneously presented on the bridge using only limited number of measuring sections of bridge bending moments. It is observed that the estimation errors of rear axle and gross weights of vehicle from both Method I and Method II can be kept smaller than 5% for considered range of noise levels using only one measuring section of bridge. It is also observed that increasing the number of measuring sections beyond 3 does not significantly improve the accuracy of weight estimation methods. Comparing between the two estimation methods, it is found that Method II yields slightly smaller errors than Method I for all considered number of measuring sections and noise levels.

4.4. Effects of Axle Spacing and Axle Weight Distribution. The effects of axle spacing and axle weight distribution of vehicle on the accuracy of weight estimation methods are investigated. The axle spacing of vehicle from 2 to 15 m and the axle weight distribution of vehicle defined by ratio of front axle weight to gross weight are varied from 20% to 80%. The vehicle having different axle spacing and axle weight distribution moving on the bridge at a constant speed of 15 m/s is simulated. The bridge surface is assumed to have the roughness of level 3. Based on the obtained bridge moments at three sections, that is, $L/3$, $L/2$, and $2L/3$, the axle weights of vehicle are estimated using Method I and Method II. Figures 9(a) to 9(c) show the estimation errors of front axle, rear axle, and gross weights of vehicle from the two methods under various axle spacing and axle weight distribution. The obtained results in Figure 9(c) clearly indicate that the estimation error of gross weight is slightly affected by both axle spacing and axle weight distribution. However, their effects on the estimation errors of front and rear axle weights as in Figures 9(a) and 9(b) are found to be significant. These errors increase as the weight of the considered axle reduces. This is mainly because the

estimation error is computed in terms of percentage error with respected to the corresponding actual weight of the axle. Therefore, with the same amount of weight error, an axle with lighter weight would give a higher percentage of error. For the gross weight estimation, the errors of gross weights from 3.9% to 5.5% and from 3.1% to 4.6% are observed using Method I and Method II, respectively. Comparing their errors, it is found that Method II yields slightly smaller errors than Method I especially for the lower axle weight distribution.

4.5. CPU Processing Time. The CPU processing time is also investigated to compare the computing speeds of Method I and Method II. Based on numerical simulation test results, the processing times required by both methods are listed in Table 4. In this study, a personal computer with Intel Core 2 Duo 2.4 GHz and 2.0 GB RAM is employed and the listed processing times are normalized by 100 data points of input bridge moment histories. The results show that Method I requires about 1–3 seconds to complete the axle weights estimation. While Method II spends up to 4–12 seconds to complete the axle loads identification. Comparing between both methods, it is clearly found that Method I exhibits about 4 times shorter processing time than Method II. However, it should be noted that Method II provides not only the axle weight information of vehicle but also its dynamic load histories.

5. Conclusions

The effectiveness of vehicle weight estimations from bridge weigh-in-motion system is studied. The measured bending moments of the instrumented bridge at selected sections under a passage of the vehicle are numerically simulated and are used as the input for vehicle weight estimations. Two weight estimation methods assuming constant magnitudes (Method I) and time-varying magnitudes (Method II) of vehicle axle loads are investigated. Their estimation accuracy are evaluated and compared under various parameters of vehicle-bridge system.

Based on the simulation results, the minimum number of bridge discretization of 4 and the minimum sampling frequency of 50 Hz are observed. It is also found that, among many considered parameters, the vehicle speed and surface roughness seem to have stronger effect on the accuracy of the two estimation methods than others. However, the estimation errors of the gross weight of vehicle can be controlled to be within ±10% if the surface roughness is kept below level 4, regardless to the vehicle speed.

It is also found from the effectiveness comparison between the two estimation methods under various vehicle and bridge conditions that Method II can provide better weight estimation than Method I for almost of the considered cases. In addition, it provides dynamic axle loads of vehicle. However, it exhibits about four times slower speed of computation than Method I.

Appendix

$$\mathbf{M_v} = \begin{bmatrix} m_v & 0 & 0 & 0 \\ 0 & I_v & 0 & 0 \\ 0 & 0 & m_1 & 0 \\ 0 & 0 & 0 & m_2 \end{bmatrix}; \qquad \mathbf{M_s} = \begin{Bmatrix} (m_1 + a_2 m_v)g \\ (m_2 + a_1 m_v)g \end{Bmatrix};$$

$$\mathbf{r}(t) = \begin{Bmatrix} r\left(x_f(t)\right) \\ r(x_r(t)) \end{Bmatrix};$$

$$\mathbf{C_v} = \begin{bmatrix} C_{S1} + C_{S2} & (-C_{S1}a_1 + C_{S2}a_2)S & -C_{S1} & -C_{S2} \\ (-C_{S1}a_1 + C_{S2}a_2)S & (C_{S1}a_1^2 + C_{S2}a_2^2)S^2 & C_{S1}a_1 S & -C_{S2}a_2 S \\ -C_{S1} & C_{S1}a_1 S & C_{S1} & 0 \\ -C_{S2} & -C_{S2}a_2 S & 0 & C_{S2} \end{bmatrix};$$

$$\mathbf{K_v} = \begin{bmatrix} K_{s1} + K_{s2} & (-K_{s1}a_1 + K_{s2}a_2)S & -K_{s1} & -K_{s2} \\ (-K_{s1}a_1 + K_{s2}a_2)S & (K_{s1}a_1^2 + K_{s2}a_2^2)S^2 & K_{s1}a_1 S & -K_{s2}a_2 S \\ -K_{s1} & K_{s1}a_1 S & K_{s1} & 0 \\ -K_{s2} & -K_{s2}a_2 S & 0 & K_{s2} \end{bmatrix};$$

$$\mathbf{C_{tt}} = \begin{bmatrix} 0 & 0 & 0 & 0 \\ 0 & 0 & 0 & 0 \\ 0 & 0 & C_{t1} & 0 \\ 0 & 0 & 0 & C_{t2} \end{bmatrix}; \qquad \mathbf{K_{tt}} = \begin{bmatrix} 0 & 0 & 0 & 0 \\ 0 & 0 & 0 & 0 \\ 0 & 0 & K_{t1} & 0 \\ 0 & 0 & 0 & K_{t2} \end{bmatrix};$$

$$\overline{\mathbf{C}}_{\mathbf{11}}(t) = \mathbf{H}(\alpha(t))\mathbf{C_t}\mathbf{H}(\alpha(t))^T; \qquad \mathbf{C_{12}}(t) = \mathbf{H}(\alpha(t))\mathbf{C}_t;$$

$$\mathbf{C_{21}}(t) = \mathbf{C_t}\mathbf{H}(\alpha(t))^T,$$

$$\overline{\mathbf{K}}_{\mathbf{11}}(t) = \mathbf{H}(\alpha(t))\mathbf{K_t}\mathbf{H}(\alpha(t))^T; \qquad \mathbf{K_{12}}(t) = \mathbf{H}(\alpha(t))\mathbf{K_t};$$

$$\mathbf{K_{21}}(t) = \mathbf{K_t}\mathbf{H}(\alpha(t))^T,$$

$$\mathbf{F_b}(t) = -\mathbf{H}(\alpha(t))\mathbf{K_t}\mathbf{r}(t) + \mathbf{H}(\alpha(t))\mathbf{M_s}, \qquad \mathbf{F_v}(t) = -\mathbf{K_t}\mathbf{r}(t). \tag{A.1}$$

Acknowledgment

The authors are very grateful to the Chulalongkorn University for the 90th year research grant for this project.

References

[1] F. Moses, "Weigh-in-motion system using instrumented bridges," *ASCE: Journal of Transportation Engineering*, vol. 105, no. 3, pp. 233–249, 1979.

[2] M. Kriss, *Weigh in motion prediction method*, M.S. thesis, Case Western Reserve University, Cleveland, Ohio, USA, 1979.

[3] N. Gagarine, *Advances in weigh-in-motion with pattern recognition and prediction of fatigue life of highway bridges*,

Ph.D. thesis, Department of Civil Engineering, University of Maryland, College Park, Md, USA, 1991.

[4] European Commission 4th Framework Programme Transport, "Weighing-in-motion of Axles and Vehicles for Europe (WAVE)," Report of Work Package, Bridge WIM systems (B-WIM), University College Dublin, 2001.

[5] S. K. Leming and H. L. Stalford, "Bridge weigh-in-motion system development using superposition of dynamic truck/static bridge interaction," in *Proceedings of the American Control Conference*, vol. 1, pp. 815–820, 2003.

[6] C. Rowley, A. Gonzalez, E. Obrien, and A. Znidaric, "Comparison of conventional and regularized bridge weigh-in-motion algorithms," in *Proceedings of the 5th International Conference on Heavy Vehicles (ICWIM '08)*, pp. 271–282, Paris, France, May 2008.

[7] S. A. Ansari, *Investigation of improved accuracy limits for dynamic bridge weigh-in-motion system*, M.S. thesis, Department of Civil Engineering, University of Maryland, College Park, Md, USA, 1990.

[8] M. I. S. Elhelbawey, *Definition of improved modeling procedures for the analysis of bridge structures under truck loading using weigh-in-motion*, Ph.D. thesis, Department of Civil Engineering, University of Maryland, College Park, Md, USA, 1991.

[9] D. R. Schelling, M. A. Sahin, M. I. Elhelbawey, S. A. Ansari, and T. E. Huang, "Definition of impact factors for bridge structure using truck loading," Research Study AW087-329-046, Maryland Department of Transportation, Brooklandville, Md, USA, 1992.

[10] S. S. Law, T. H. T. Chan, and Q. H. Zeng, "Moving force identification: a time domain method," *Journal of Sound and Vibration*, vol. 201, no. 1, pp. 1–22, 1997.

[11] S. S. Law, T. H. T. Chan, and Q. H. Zeng, "Moving force identification a frequency and time domains analysis," *Journal of Dynamics Systems, Measurement, and Control*, vol. 121, no. 3, pp. 394–401, 1999.

[12] X. Q. Zhu and S. S. Law, "Identification of vehicle axle loads from bridge dynamic responses," *Journal of Sound and Vibration*, vol. 236, no. 4, pp. 705–724, 2000.

[13] L. Yu and T. H. T. Chan, "Moving force identification from bending moment responses of bridge," *Structural Engineering and Mechanics*, vol. 14, no. 2, pp. 151–170, 2002.

[14] X. Q. Zhu and S. S. Law, "Moving loads identification through regularization," *Journal of Engineering Mechanics*, vol. 128, no. 9, pp. 989–1000, 2002.

[15] S. S. Law, J. Q. Bu, X. Q. Zhu, and S. L. Chan, "Vehicle axle loads identification using finite element method," *Engineering Structures*, vol. 26, no. 8, pp. 1143–1153, 2004.

[16] S. S. Law and Y. L. Fang, "Moving force identification: optimal state estimation approach," *Journal of Sound and Vibration*, vol. 239, no. 2, pp. 233–254, 2001.

[17] T. Pinkaew, "Identification of vehicle axle loads from bridge responses using updated static component technique," *Engineering Structures*, vol. 28, no. 11, pp. 1599–1608, 2006.

[18] T. Pinkaew and P. Asnachinda, "Experimental study on the identification of dynamic axle loads of moving vehicles from the bending moments of bridges," *Engineering Structures*, vol. 29, no. 9, pp. 2282–2293, 2007.

[19] X. Q. Zhu and S. S. Law, "Moving forces identification on a multi-span continuous bridge," *Journal of Sound and Vibration*, vol. 228, no. 2, pp. 377–396, 1999.

[20] X. Q. Zhu and S. S. Law, "Orthogonal function in moving loads identification on a multi-span bridge," *Journal of Sound and Vibration*, vol. 245, no. 2, pp. 329–345, 2001.

[21] X. Q. Zhu and S. S. Law, "Moving load identification on multi-span continuous bridges with elastic bearings," *Mechanical Systems and Signal Processing*, vol. 20, no. 7, pp. 1759–1782, 2006.

[22] T. H. T. Chan and D. B. Ashebo, "Theoretical study of moving force identification on continuous bridges," *Journal of Sound and Vibration*, vol. 295, no. 3–5, pp. 870–883, 2006.

[23] T. H. T. Chan and D. B. Ashebo, "Moving axle load from multi-span continuous bridge: laboratory study," *Journal of Vibration and Acoustics, Transactions of the ASME*, vol. 128, no. 4, pp. 521–526, 2006.

[24] "Optimization toolbox for use with MATLAB," The MathWorks, Inc., Natick, Mass, USA, 2001, http://www.mathworks.com/.